16th International Symposium on Particles Strings and Cosmology (PASCOS 2010) IOP Publishing
Journal of Physics: Conference Series **259** (2010) 012066 doi:10.1088/1742-6596/259/1/012066

Dark matter in minimal supergravity with type-II seesaw

J. N. Esteves

E-mail: joaomest@cftp.ist.utl.pt
Departamento de Física and CFTP, Instituto Superior Técnico
Av. Rovisco Pais 1, 1049-001 Lisboa, Portugal

Abstract. We calculate the relic density of the lightest neutralino in a supersymmetric seesaw type-II ("triplet seesaw") model with minimal supergravity boundary conditions at the GUT scale. The presence of a triplet below the GUT scale, required to explain measured neutrino data in this setup, leads to a characteristic deformation of the sparticle spectrum with respect to the pure mSugra expectations, affecting the calculated relic dark matter (DM) density. We discuss how the DM allowed regions in the $(m_0, M_{1/2})$ plane change as a function of the (type-II) seesaw scale. We also compare the constraints imposed on the models parameter space form upper limits on lepton flavour violating (LFV) decays to those imposed by DM.

1. Introduction

Standard cosmology requires the existence of a non-baryonic dark matter (DM) contribution to the total energy budget of the universe. In the past few years estimates of the DM abundance have become increasingly precise. Indeed, the Particle Data Group now quotes at 1 σ c.l. [1]

$$\Omega_{DM} h^2 = 0.105 \pm 0.008. \tag{1}$$

Neutrino oscillation experiments have shown that neutrinos have non-zero mass and mixing angles and the most recent global fits to all data [2] confirm again that the mixing angles are surprisingly close to the so-called tri-bimaximal mixing (TBM) values [3]. It was shown long ago that if neutrinos are Majorana particles, their mass is described by a unique dimension-5 operator [4]

$$m_\nu = \frac{f}{\Lambda}(HL)(HL). \tag{2}$$

All (Majorana) neutrino mass models reduce to this operator at low energies. Assuming complete flavour blindness in the soft supersymmetry breaking parameters at some large scale, the neutrino Yukawa matrices will, in general, lead to non-zero flavour violating entries in the slepton mass matrices, if the seesaw scale is lower than the scale at which SUSY is broken. This was first pointed out in [5].

In this work [7] we studied neutralino dark matter within a supersymmetric type-II seesaw model with mSugra boundary conditions. For definiteness, the model we consider consists of the MSSM particle spectrum to which we add a single pair of **15**- and $\overline{\mathbf{15}}$-plets. This is the simplest supersymmetric type-II setup, which allows one to maintain gauge coupling unification [6] and explain measured neutrino oscillation data.

In mSugra - assuming a standard thermal history of the early universe - only four very specific regions in parameter space can correctly explain the most recent WMAP data [8]. These are (i) the bulk region; (ii) the co-annihilation line; (iii) the "focus point" line and (iv) the "higgs funnel" region. More details can be found on [7].

2. Setup: mSugra and $SU(5)$ motivated type-II seesaw

We will always refer to minimal Supergravity (mSugra) as the "standard" against which we compare all our results. The model consists in extending the MSSM particle spectrum by a pair of **15** and $\overline{\mathbf{15}}$. It is the minimal supersymmetric seesaw type-II model which maintains gauge coupling unification [6].

One of the triplets in the model described in [6] has the correct quantum numbers to generate neutrino masses. Integrating out the heavy triplets at their mass scale a dimension-5 operator of the form eq. (2) is generated and after electro-weak symmetry breaking the resulting neutrino mass matrix can be written as

$$m_\nu = \frac{v_2^2}{2}\frac{\lambda_2}{M_T}Y_T. \tag{3}$$

Here v_2 is the vacuum expectation value of Higgs doublet H_2 and we use the convention $\langle H_i\rangle = \frac{v_i}{\sqrt{2}}$. m_ν can be diagonalized in the standard way with a unitary matrix U, containing in general 3 angles and 3 phases. Note that $\hat{Y}_T = U^T \cdot Y_T \cdot U$ is diagonalized by *the same matrix as* m_ν. This means that if all neutrino eigenvalues, angles and phases were known, Y_T would be completely fixed up to an overall constant, which can be written as $\frac{M_T}{\lambda_2} \simeq 10^{15}\text{GeV}\ \left(\frac{0.05\text{ eV}}{m_\nu}\right)$. Thus, current neutrino data requires M_T to be lower than the GUT scale by (at least) an order or magnitude.

The full set of RGEs for the **15** + $\overline{\mathbf{15}}$ can be found in [6] and in the numerical calculation, presented in the next section, we solve the exact RGEs.

3. Numerical results

In this section we discuss our numerical results. All the plots shown below are based on the program packages SPheno [12] and micrOMEGAs [14, 13]. We use SPheno V3 [15], including the RGEs for the **15** + $\overline{\mathbf{15}}$ case [6, 16] at the 2-loop level for gauge couplings and gaugino masses and at one-loop level for the remaining MSSM parameters and the 15-plet parameters, for a discussion see [16]. For any given set of mSugra and 15-plet parameters SPheno calculates the supersymmetric particle spectrum at the electro-weak scale, which is then interfaced with micrOMEGAs2.2 [17] to calculate the relic density of the lightest neutralino, $\Omega_{\chi_1^0}h^2$. A sketch of the all process can be seen in fig.(1).

For the standard model parameters we use the PDG 2008 values [1], unless specified otherwise. As discussed below, especially important are the values (and errors) of the bottom and top quark masses, $m_b = 4.2 + 0.17 - 0.07$ GeV and $m_t = 171.2 \pm 2.1$ GeV. Note, the m_t is understood to

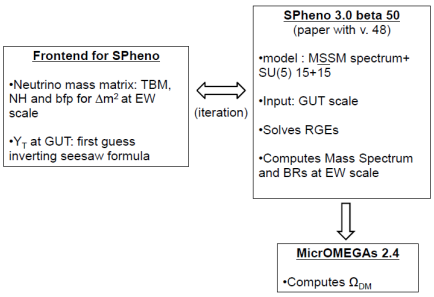

Figure 1. Dark Matter computation.

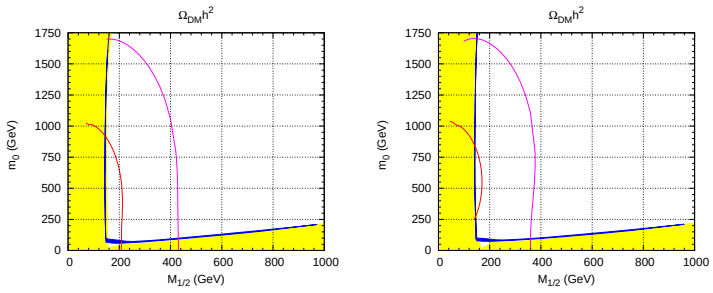

Figure 2. Limits for mSugra with $\tan\beta = 10$, and $\mu > 0$ for $A_0 = -300$ GeV (left panel) and $A_0 = -500$ GeV (right panel). The blue regions are allowed by the DM constraint The yellow bounds refer to the $\widetilde{\tau}$ being the LSP (bottom) and to the LEP bound on the chargino mass (left).

be the pole-mass and $m_b(m_b)$ is the $\overline{MS}$ mass. As the allowed range for $\Omega_{DM}h^2$ we always use the 3 σ c.l. boundaries as given in [1], i.e. $\Omega_{DM}h^2 = [0.081, 0.129]$. Note, however that the use of 1 σ contours results in very similar plots, due to the small error bars.

We define our "standard choice" of mSugra parameters as $\tan\beta = 10$, $A_0 = 0$ and $\mu > 0$ and use these values in all plots, unless specified otherwise. We then show our results in the plane of the remaining two free parameters, $(m_0, M_{1/2})$.

In fig. (2) we show two examples for the DM allowed region and the regions disfavored by the Higgs boson mass bound at $m_{h^0} = 114.4$ GeV and $m_{h^0} = 110$ GeV. Larger negative A_0 leads to a less stringent constraint (for $\mu > 0$). Note, that all of the bulk region becomes allowed at $A_0 = -500$ GeV, once the theoretical uncertainty in the Higgs boson mass calculation is taken into account.

We now turn to a discussion of large $\tan\beta$. At large values of $\tan\beta$ the width of the CP-odd Higgs boson A becomes large, $\Gamma_A \sim M_A \tan^2\beta(m_b^2 + m_t^2)$, and a wide s-channel resonance occurs in the region $m_{\chi_1^0} \simeq M_A/2$. The enhanced annihilation cross section reduces $\Omega_{\chi_1^0}h^2$ to acceptable levels, the resulting region is known as the "higgs funnel" region.

The higgs funnel is very sensitive to the exact value of $\tan\beta$ and to the values (and errors) of the top and bottom quark mass. The position of the funnel is especially sensitive to the exact value of m_b. However, future determinations of m_b and m_t could improve the situation considerably.

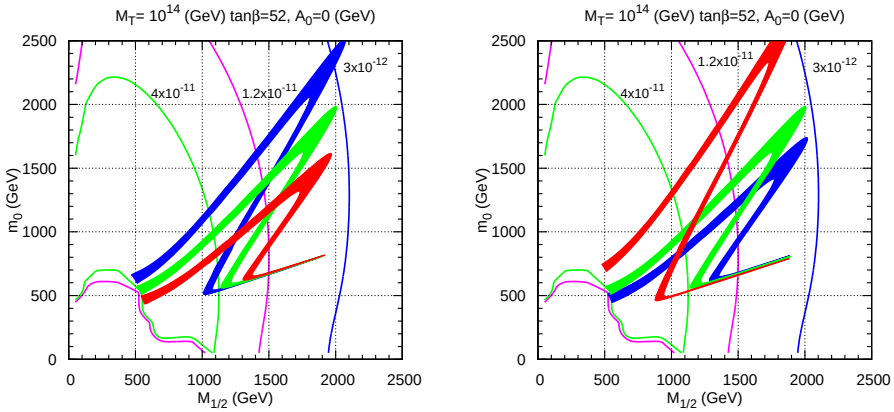

Figure 3. Allowed region for the dark matter density in the $(m_0, M_{1/2})$ plane for $A_0 = 0$, $\mu \geq 0$ and $\tan\beta = 52$, for $M_T = 10^{14}$ GeV and (to the left) for three values of $m_{top} = 169.1$GeV (blue), $m_{top} = 171.2$ GeV (green) and $m_{top} = 173.3$ GeV (red). To the right: The same, but varying m_b. $m_{bot} = 4.13$ GeV (blue), $m_{bot} = 4.2$ GeV (green) and $m_{bot} = 4.37$ GeV (red). Superimposed are contour levels for $\mathrm{Br}(\mu \to e\gamma)$

In the numerical calculation we have chosen neutrino masses to be of the normal hierarchical type and fitted the neutrino angles to exact tri-bimaximal (TBM) values [3], i.e. $\tan^2\theta_{\mathrm{Atm}} = 1$, $\tan^2\theta_{\odot} = 1/2$ and $\sin^2\theta_{\mathrm{R}} = 0$. This has to be done in a simple iterative procedure, since the triplet parameters are defined at the high scale, whereas neutrino masses and angles are measured at low scale. For more details on the fit procedure see [16].

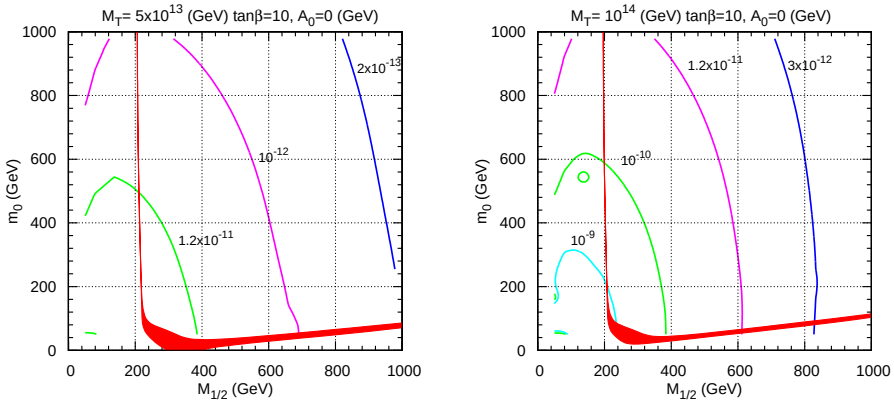

Figure 4. Limits for mSugra with $\tan\beta = 10$, $\mu > 0$ and $A_0 = 0$ GeV for $M_T = 5 \times 10^{13}$ GeV (left panel) and $M_T = 10^{14}$ GeV (right panel). Contour levels for $\mathrm{Br}(\mu \to e\gamma)$ are also shown.

Finally, we will compare the constraints imposed on the parameter space of the model by $\Omega_{DM}h^2$ with the constraints from the current data on non-observation of lepton flavour violating processes. Since LFV within the present model has been studied in some detail in [16], we will not repeat all of the discussion here. Instead, here we concentrate on $\mu \to e\gamma$ exclusively, since the upper bound on $Br(\mu \to e\gamma)$ of $Br(\mu \to e\gamma) \leq 1.2 \cdot 10^{-11}$ [1] has been shown to provide currently the most important constraint.

In fig. (4) we show the DM allowed parameter regions for $\tan\beta = 10$ and two values of M_T,

$M_T = 5 \cdot 10^{13}$ GeV (to the left) and $M_T = 10^{14}$ GeV (to the right), for a fixed choice of all other parameters. Superimposed on this plot are lines of constant branching ratio for $Br(\mu \to e\gamma)$. The latter have been calculated requiring neutrino masses being hierarchical and fitted to solar and atmospheric neutrino mass squared differences and neutrino angles fitted to TBM values. Within the $(m_0, M_{1/2})$ region shown, $Br(\mu \to e\gamma)$ can vary by two to three orders of magnitude, depending on the exact combination of $(m_0, M_{1/2})$, even for all other parameters fixed. The most important parameter determining $Br(\mu \to e\gamma)$, once neutrino data is fixed, however, is M_T, as can be seen comparing the figure to the left with the plot on the right. While for $M_T = 10^{14}$ GeV about "half" of the plane is ruled out by the non-observation of $\mu \to e\gamma$, for $M_T = 5 \cdot 10^{13}$ GeV with the current upper limit nearly all of the plane becomes allowed. The strong dependence of $\mu \to e\gamma$ on M_T can be understood from the analytical formulas presented in [16]. In this paper it was shown that $Br(\mu \to e\gamma)$ scales very roughly as $Br(\mu \to e\gamma) \propto M_T^4 \log(M_T)$, if neutrino masses are to be explained correctly. For $\tan\beta = 10$ one thus concludes that with present data values of M_T larger than (few) 10^{13} GeV - (few) 10^{14} GeV are excluded by $Br(\mu \to e\gamma)$, to be compared with $M_T/\lambda_2 \lesssim 10^{15}$ GeV from the measured neutrino masses. Note, however, that (i) the constraint from neutrino masses is relatively independent of $\tan\beta$, m_0 and $M_{1/2}$, while $\mu \to e\gamma$ shows strong dependence on these parameters; and (ii) allowing the value of the reactor angle $\sin^2\theta_{\rm R}$ to vary up to its experimental upper limit, $\sin^2\theta_{\rm R} = 0.056$ [2], leads to larger values of $Br(\mu \to e\gamma)$ and thus to a tighter upper limit on M_T.

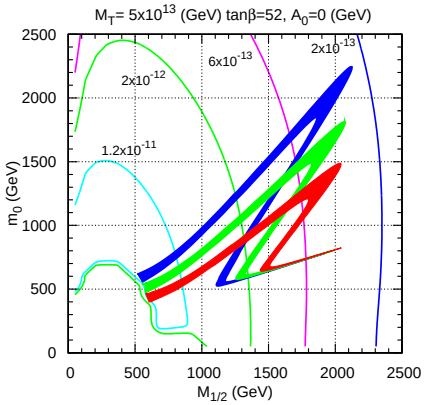

Figure 5. Allowed region for dark matter density ($0.081 < \Omega_{\chi_1^0} h^2 < 0.129$) in the $(m_0, M_{1/2})$ plane for $A_0 = 0$, $\mu \geq 0$ and $\tan\beta = 52$, for three values of $m_{top} = 169.1$ GeV (blue), $m_{top} = 171.2$ GeV (green) and $m_{top} = 173.3$ GeV (red) for $M_T = 5 \times 10^{13}$. Superimposed are the contour lines for the $Br(\mu \to e\gamma)$.

In figs. (3) and (5) we show the results for a calculation comparing dark matter and LFV in the case of large $\tan\beta$. Here the same constraints as in fig. (4) are shown, however for $\tan\beta = 52$. Again we show the calculation for two values of M_T, since M_T is the most important free parameter. It is known that at large values of $\tan\beta$, LFV decays are enhanced due to an enhanced chargino diagram, which in the limit of large $\tan\beta$ scales approximately as $\tan^2\beta$ [18]. Therefore, constraints on the parameter space from non-observation of LFV decays are more severe in case of large $\tan\beta$, leading to tighter upper limits on M_T. This is clear if we compare fig. (4) on one side and figs. (3) and (5) on the other, noticing the different scales. However, because of the higgs funnel region developing for large $\tan\beta$, the interesting part of the parameter

space enlarges compensating for the larger values of the LFV decays. This can be seen in fig. (5), where for $M_T = 5 \times 10^{13}$ GeV (left), most of the $(m_0, M_{1/2})$ plane is allowed by the upper limit on $Br(\mu \to e\gamma)$, while in fig. (3), left, for $M_T = 10^{14}$ GeV about "half" of the plane is ruled out by this limit.

Acknowledgments

J. N. Esteves wishes to thank M. Hirsch, S. Kaneko, W. Porod and J. C. Romao for a fruitful collaboration that leaded to the work [7] that was presented here.

References

[1] C. Amsler et al., Physics Letters B667, 1 (2008); http://pdg.lbl.gov/
[2] For a review of neutrino oscillation data, see: M. Maltoni, T. Schwetz, M. A. Tortola and J. W. F. Valle, New J. Phys. **6**, 122 (2004); an updated analysis has now been published in T. Schwetz, M. Tortola and J. W. F. Valle, New J. Phys. **10**, 113011 (2008) (*Preprint* arXiv:0808.2016 [hep-ph]) where all experimental references can be found.
[3] P. F. Harrison, D. H. Perkins and W. G. Scott, Phys. Lett. **B530**, 167 (2002) (*Preprint* hep-ph/0202074)
[4] S. Weinberg, Phys. Rev. Lett. **43**, 1566 (1979); S. Weinberg, Phys. Rev. D **22**, 1694 (1980)
[5] F. Borzumati and A. Masiero, Phys. Rev. Lett. **57**, 961 (1986)
[6] A. Rossi, Phys. Rev. D **66**, 075003 (2002) (*Preprint* hep-ph/0207006)
[7] J. N. Esteves, S. Kaneko, J. C. Romao, M. Hirsch and W. Porod, Phys. Rev. D **80** (2009) 095003 (*Preprint* arXiv:0907.5090 [hep-ph])
[8] E. Komatsu *et al.* [WMAP Collaboration], Astrophys. J. Suppl. **180**, 330 (2009) (*Preprint* arXiv:0803.0547 [astro-ph])
[9] B. C. Allanach, G. Belanger, F. Boudjema and A. Pukhov, JHEP **0412**, 020 (2004) (*Preprint* hep-ph/0410091)
[10] H. Baer, C. Balazs and A. Belyaev, JHEP **0203**, 042 (2002) (*Preprint* hep-ph/0202076)
[11] J. L. Feng, K. T. Matchev and T. Moroi, Phys. Rev. D **61**, 075005 (2000) (*Preprint* hep-ph/9909334)
[12] W. Porod, Comput. Phys. Commun. **153**, 275 (2003) (*Preprint* hep-ph/0301101)
[13] G. Belanger, F. Boudjema, A. Pukhov and A. Semenov, Comput. Phys. Commun. **176**, 367 (2007) (*Preprint* hep-ph/0607059)
[14] G. Belanger, F. Boudjema, A. Pukhov and A. Semenov, Comput. Phys. Commun. **174**, 577 (2006) (*Preprint* hep-ph/0405253)
[15] The latest version of SPheno can be obtained from: http://theorie.physik.uni-wuerzburg.de/ porod/SPheno.html
[16] M. Hirsch, S. Kaneko and W. Porod, Phys. Rev. D **78**, 093004 (2008) (*Preprint* arXiv:0806.3361 [hep-ph])
[17] http://wwwlapp.in2p3.fr/lapth/micromegas/
[18] J. Hisano, T. Moroi, K. Tobe and M. Yamaguchi, Phys. Rev. D **53**, 2442 (1996) (*Preprint* hep-ph/9510309)